Ultra-sensitive and wide-dynamic-range sensors based on dense arrays of carbon nanotube tips

Sun, Gengzhi; Huang, Yinxi; Zheng, Lianxi; Zhan, Zhaoyao; Zhang, Yani; Pang, John Hock Lye; Wu, Tom; Chen, Peng

2011

Sun, G., Huang, Y., Zheng, L., Zhan, Z., Zhang, Y., Pang, J. H. L., et al. (2011). Ultra-sensitive and wide-dynamic-range sensors based on dense arrays of carbon nanotube tips. Nanoscale, 3, 4854-4858.

https://hdl.handle.net/10356/94378

https://doi.org/10.1039/c1nr10899a

Nanoscale

Dynamic Article Links ►

Cite this: DOI: 10.1039/c0xx00000x

www.rsc.org/xxxxxx

ARTICLE TYPE

Ultra-sensitive and wide-dynamic-range sensors based on dense arrays of carbon nanotube tips†

Gengzhi Sun,[a] Yinxi Huang,[b] Lianxi Zheng,*[a] Zhaoyao Zhan,[a] Yani Zhang,[a] John H. L. Pang,[a] Tom Wu[c] and Peng Chen[b]

Received (in XXX, XXX) Xth XXXXXXXXX 20XX, Accepted Xth XXXXXXXXX 20XX
DOI: 10.1039/b000000x

Electrochemical electrodes based on dense and vertically aligned arrays of multi-walled carbon nanotubes (MWCNTs) were produced. The open tips of individual hollow nanotubes are exposed as active sites while the entangled nanotube stems encapsulated in epoxy collectively provide multiplexed and highly conductive pathways for charge transport. This unique structure together with the extraordinary electrical and electrochemical properties of MWCNTs offers a high signal-to-noise ratio (thus high sensitivity) and a large detection range, compared with other carbon-based electrodes. Our electrodes can detect K_3FeCN_6 and dopamine at concentrations as low as 5 nM and 10 nM, respectively, and are responsive in a large dynamic range that spans almost 5 orders of magnitude.

1. Introduction

With the unique combination of their one-dimensional structure and extraordinary electronic properties, carbon nanotubes (CNTs) have been demonstrated to have superior abilities for sensor applications,[1–4] especially the electrochemical sensor applications.[4–8] In most electrochemical studies, random thin-film networks of CNTs were used to modify electrode surfaces for detecting various chemical and biological targets.[5,9–11] The superior performance of such CNT-modified electrodes over conventional planar electrodes is because the CNT networks facilitate the electron transfer and provide a large effective surface area due to the extremely high surface-to-volume ratio of CNTs.[12] But an increased detection area also means a higher background current or noise. Furthermore, the raw CNT materials used in most studies either have a high content of impurities or are bundled together, and then the purification and dispersion processes must be employed.[13,14] These processes inevitably introduce defects on CNTs, and thus degrade CNT's electrochemical performances[15] because of the increased resistance and capacitance resulting from the high defect density.[16]

Nanoelectrodes offer various benefits compared to the planar macro-electrodes or micro-electrodes. Theoretically, they should exhibit a high signal-to-noise ratio and an enhanced detection limit, because the noise arising from double layer capacitance diminishes more quickly with the shrinking area although the signal decreases linearly with the area. Another advantage of the nanoelectrodes arises from the radial (3 dimensional) diffusion to the point-like electrode, which leads to increased mass transport.[15,17] Several techniques have been developed to fabricate nanosized electrochemical probes. Among them, the smallest are single CNT electrodes, which have demonstrated their excellent sensitivity.[18,19] However, it is extremely challenging to fabricate such single CNT electrodes and insulate their non-active areas. And the small current generated by a single nanoelectrode is difficult to be measured by the conventional instruments.

Attempts have also been made to fabricate CNT arrays as the electrochemical electrodes. These methods involve non-trivial patterning,[20–23] growth,[24] and fabrication processes.[21,24,25] Significant progress has been made, but it is still challenging to obtain a low detection limit and a large dynamic range from the same electrode. In this study, we used as-grown vertically aligned CNT arrays to constitute a novel electrode structure, in which only the open tips of CNTs on the top of the electrodes are active sites, while the entire CNT array collectively acts as the current transport path. The signal generated at any individual CNT tip could be transported by such a multiplexed network because of the entangled nature of individual CNTs within the array. In addition, as-grown CNTs without any treatment are used to ensure minimum defects. Since all individual CNTs are well insulated except their open tips, this type of CNT array electrode (CNTAE) promises a high signal-to-noise ratio due to the small reactive areas of the open tips, but still retains a signal current as high as that of a bulk electrode due to the fast mass transfer rate to individual CNTs, the fast heterogeneous electron transfer, and the extremely conductive network for current transport. Moreover, the easy synthesis of CNT arrays and simple fabrication

[a]*School of Mechanical and Aerospace Engineering, Nanyang Technological University, 50 Nanyang Avenue, Singapore 639798. E-mail: lxzheng@ntu.edu.sg; Fax: +65-6792-4062; Tel: +65-6790-4163*
[b]*School of Chemical and Biomedical Engineering, Nanyang Technological University, 70 Nanyang Drive, Singapore 637457*
[c]*School of Physical and Mathematical Sciences, Nanyang Technological University, 21 Nanyang Link, Singapore 637371*

processes of the CNTAEs make them promising to commercially scale-up.

2. Experimental

2.1. Sample preparation

Vertically aligned CNT arrays were grown by a chemical vapor deposition (CVD) process which is similar to the method we reported previously.[26] During the CNT growth, pure acetylene (C_2H_2) was used as the carbon source, and the forming gas, argon (Ar) and hydrogen (H_2), served as the carrier gas. The catalyst used in this study was Fe (0.8 nm) layer, which was deposited by the electron-beam deposition technique on a Si wafer with a 2 μm SiO_2 layer. Typically, the CNT growth was carried out at 750 °C for 20 min with a 200 sccm total flow gas.

For realizing an electrical connection and conducting electrochemical measurements, a Cu strip was first connected with the top of a CNT array using silver paste. After being removed from the Si substrate, the CNT array was then infiltrated by epoxy resin (Electron Microscopy Sciences, EPO-FIX) to fill the interstitial spaces between the individual CNTs. The infiltration process was performed for 3 hours in a vacuum chamber at a pressure of 10 mTorr to get rid of air bubbles from the epoxy mixture, and also help the liquid-state monomers seamlessly infiltrate into the empty spaces between the individual CNTs. After the monomer infiltration, the composite was left in an oven for post cure to further insulate the structure and also provide a good mechanical support for the CNTs. After these steps, mechanical polishing was used to break the top part of the CNTs and expose their open tips. Finally, the sample was rinsed with de-ionized water. Fig. 1a shows a schematic structure of the as-prepared CNTAE. The circles drawn on the top surface show the exposed open tips, and the entangled lines represent embedded individual CNTs. The fabrication processes of the CNTAEs are illustrated in Fig. 1b. The fabrication of the CNT array electrode is very process dependent. There are several other important parameters involved in the fabrication process which will influence the yield of the array electrode, for instance: the properties of epoxy, the site density of CNTs in the array, the diameters of CNTs, the thickness of CNT arrays, the vacuum conditions and the polymerization conditions.

2.2. Characterization methods

Transmission electron microscope (TEM) imaging of the CNTs was performed in a JEOL 2010 TEM. After 30 minutes of sonication in an ultrasonic bath cleaner, a droplet of the CNT dispersion was cast onto a TEM copper grid and the solvent was evaporated overnight at the room temperature. Raman scattering was obtained from a Reinshaw's inVia Raman Spectroscope with a 633 nm He–Ne laser source. The surface morphology information of the CNTAEs was acquired by an atomic force microscope (AFM, Digital Instrument, S3000).

Electrochemical characterization was performed with a CHI 760 electrochemical station. A one-compartment cell was used with a platinum wire as the auxiliary electrode and Ag/AgCl (saturated KCl aqueous solution) as the reference electrode. The cyclic voltammetry (CV) of K_3FeCN_6 and K_4FeCN_6 was used for the characterization of the CNTAE. The amperometric method was employed for dopamine (DA) quantification. The DA solution was prepared freshly and added into a phosphate buffer solution (PBS) successively with a fixed applied potential at 0.7 V.

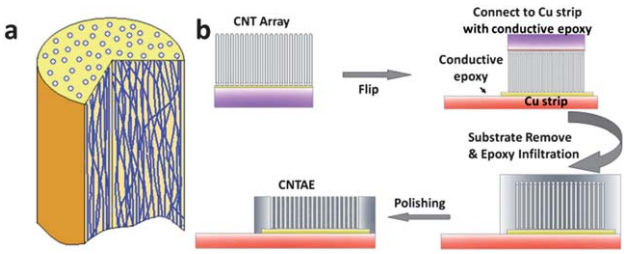

Fig. 1 Structure and fabrication of a CNTAE. (a) Schematic structure of the open-tip CNTAE. (b) Schematic fabrication procedures of the CNTAE.

3. Results and discussion

3.1. Properties of the CNT arrays

Fig. 2a is a typical scanning electron microscopy (SEM) image in which an array with a thickness of about 450 μm is shown. Fig. 2b is a magnified side-view SEM image of this CNT array, showing that the individual CNTs are entangled with each other but roughly aligned along the vertical direction. The detailed structures of the individual CNTs have been studied by TEM, and typical TEM images are presented in Fig. 2c and its inset. The as-grown CNTs are multi walled with a mean diameter of 10.5 nm and an average wall number of 6. The Raman spectrum of the array is shown in Fig. 2d, with the expected D and G bands located at 1330 and 1580 cm^{-1}, respectively. The G/D ratio is about 1.3, which is higher than our previous result,[26] indicating a better CNT quality.

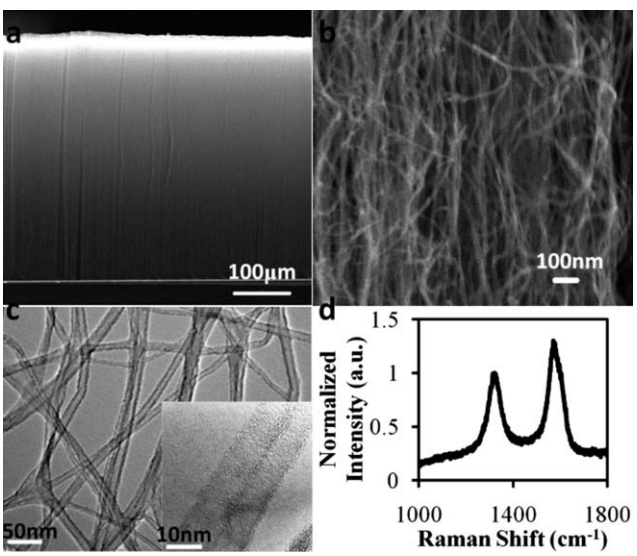

Fig. 2 Characterization of as-grown CNT arrays. (a) SEM image of the CNT array. (b) Magnified side-view SEM image of the CNT array. (c) TEM image of the individual CNTs (inset is a high resolution TEM image). (d) Raman spectrum of the CNT array.

3.2. Morphological and electrical properties of the CNTAEs

The top surfaces of fabricated CNTAEs have been studied by AFM, and the typical topography is shown in Fig. 3a. It is clearly shown that only the open tips (circles) of the embedded CNTs are exposed. For visual guidance, some open tips are highlighted with blue circles in a magnified AFM image (Fig. 3b). From these AFM images, we could find that CNTs in the electrode have a site density of about 5×10^{10} cm^{-2} with an average interspacing of 45 nm between the individual CNTs. The density is higher than that of the arrays grown from PECVD.[21,24] To further prove that these circles are open tips of the CNTs, we coat Cu nanoparticles on the top surface of one CNTAE using an electrodeposition technique, a method similar to that reported by R. M. Penner.[27,28] Fig. 3c is an AFM image scanned after Cu nanoparticles being coated, and it shows that the whole surface is almost completely covered by Cu nanoparticles. Since only the CNTs are conductive in this composite structure, the success of the Cu coating through the electrodeposition implies that these circle-like structures are indeed the open tips of CNTs.

To characterize the conductivity of the CNTAE in the vertical direction, a thin layer of gold was deposited on the top surface of the CNTAE. Current–voltage (I–V) characteristics were obtained, as shown in Fig. 3d, using a two-probe method by sweeping the bias voltage between −0.1 and +0.1 V. A linear and symmetric dependence of current on voltage was observed, confirming an ohmic contact between the CNT array and the Cu strip. For the assembly with an area of 3 mm^2, the total resistance is 11.9 Ω, indicating a good electrical property of the CNTAE in the vertical direction and a good electrical connection between the CNT array and the Cu strip.

3.3. Electrochemical properties of the CNTAEs

For the electrochemical validation, a CNTAE with a surface area of 30 mm^2 was first studied in 0.1 M KCl which served as the supporting electrolyte. Since the background current, which is proportional to the effective double layer capacitance (or effective active area), determines the signal-to-noise ratio (or sensitivity) of an electrode, we compared the background currents of this electrode with a standard glass carbon electrode (GCE). As shown in Fig. 4a, the background current of this CNTAE is about 6.7×10^{-11} A mm^{-2}, which is two orders of magnitude lower than that of the GCE (1.4×10^{-8} A mm^{-2}). Based on the fact that the site density of the as-grown CNT array is 5×10^{10} cm^{-2}, it is estimated that the effective double layer capacitance (thus noise) contributed from a single CNT with a diameter of 10.5 nm is much smaller than that of a disc with the same diameter, and it is similar to that from a nano-ring with an outer diameter of 10.5 nm and an inner diameter of 9.8 nm. Fig. 4b shows the typical cyclic voltammetry (CV) measurements recorded at a potential sweep rate of 50 mV s^{-1} for K_3FeCN_6 at concentrations of 5 nM, 10 nM, 50 nM, 98 nM and 238 nM. Evidently, the response for a concentration of 5 nM is easily discernible. We have conducted the CV measurements in a wide range of concentrations, and found that the peak current for the reduction of K_3FeCN_6 is roughly linear with the concentration over the range of 1 μM to 300 μM, but follows a power law with an exponent of about 0.35 ($I \propto C^{0.35}$) when the concentration is lower than 1 μM, as shown in Fig. 4c. The total responsive concentration range is almost 5 orders of magnitude. A weak dependence of the signal at low concentration range has also been observed in other nanoelectrode arrays and has been explained by a surface adsorption effect.[29] Fig. 4d shows that the peak current is linear with the square root of the scan rate, suggesting that the reaction is controlled by a semi-infinite linear diffusion.

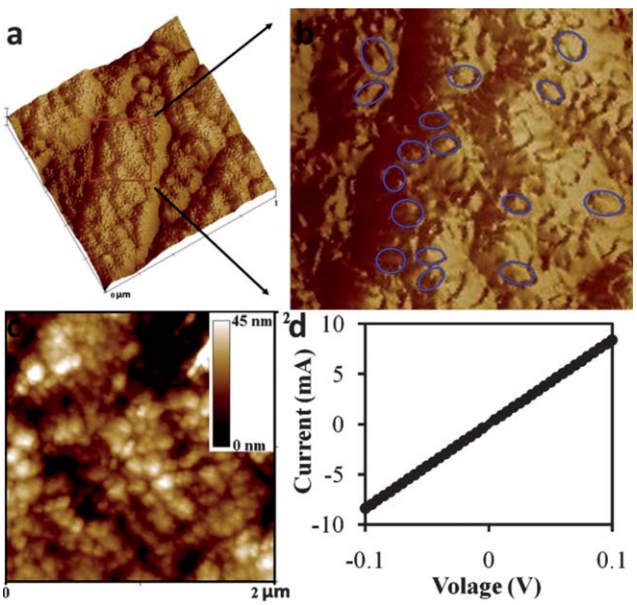

Fig. 3 Morphological and electrical properties of the CNTAE. (a) AFM image of the top surface of an as-prepared CNTAE. (b) Enlarged AFM image with highlighted open tips of the CNTs. (c) AFM image of the CNTAE surface after being coated with a layer of Cu nanoparticles. (d) I–V curve of the CNTAE.

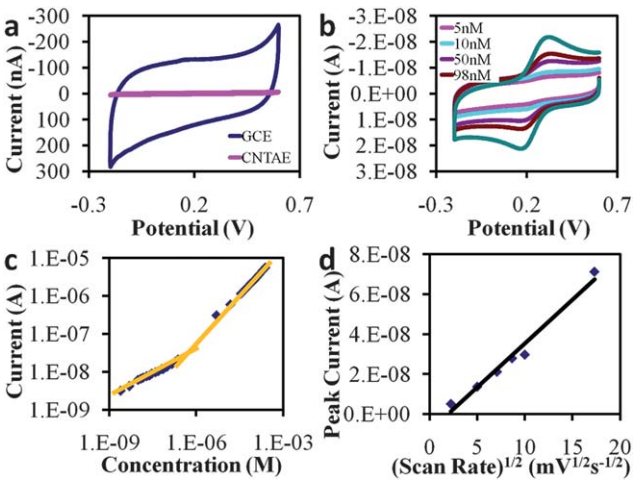

Fig. 4 Electrochemical properties of the CNTAE. (a) Background currents of the CNTAE and the GCE. (b) CV measurements of the CNTAE at different concentrations. (c) Relationship between the peak current of the CNTAE and the concentration of the analyte. (d) Dependence of the peak current on the scan rate.

Since single discrimination against the background current is a key challenge in the use of amperometry for trace level analysis, we compare the performance of our electrodes with those in previous reports in terms of the background current and the signal current, and show the results in Fig. 5a. The data for other electrode structures, including macroelectrodes, microelectrodes, and electrode arrays, are collected and/or calculated (normalized to a concentration of 100 μM) from the literature.[20,30–37] It is found that the signal current of our CNTAE electrode is close to that of the large macroelectrodes (at μA level) but the background current is comparable with that of a single microelectrode. Our CNTAE offers an ultrahigh sensitivity and a wide detection range, compared to other existing electrode structures. We believe that three factors of the structural uniqueness contribute to these superior performances: (1) The active sites are open tips of the CNTs. It is believed that the open tips are much more active for the electron transfer reactions than the sidewall of CNTs.[12] And the non-active parts are well-insulated by the epoxy without contributing to the double-layer capacitance (thus noise). This structure offers the benefit for high sensitive detections. (2) The total electrochemical reactive area is very small because only those CNT open tips working as nano-ring electrodes are exposed to the analyte. It is well known that the mass transfer process of the analyte at the surface of the working electrodes depends on the geometry of the electrodes. For example, when using a macro/micro-disk electrode as the working electrode, the current density is not uniform across the surface of the disk but greater at the edges, because these edges offer the nearest point of arrival to the electroreactant drawn from a large surrounding volume.[6,17,38] Here, in our case, the individual electrodes are even smaller down to nano-scale, and the geometry of each electrode is a nanoring, therefore, these edges offer the best active sites for electrochemical reactions as the mass transfer is faster than that at the planar electrode. This is one of the reasons that our CNTAEs exhibit such a high sensitivity. For a dense nanoelectrode array, it has been also proven that the Faradic current is proportional to the total geometric area (A_{geom}; *e.g.*, nanodisc plus insulator area) of the nanoelectrode array, whereas the background current is proportional to the sum of the areas of the electrode elements in the nanoelectrode array (A_{act}, active area).[17,38,39] This offers the opportunity that a large detection range could be realized. (3)

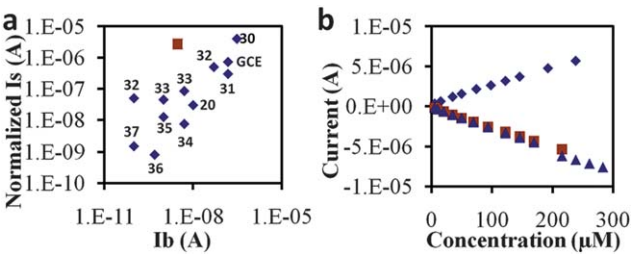

Fig. 5 (a) Comparison between the CNTAE and other electrode structures (the red square represents our CNTAE, and the blue diamonds represent data from references indicated by labelled numbers and data from a GCE in this report). (b) CV peak currents at different concentrations after being polished (blue diamond: first polish, blue triangle: second polish, and red square: third polish), showing a good repeatability.

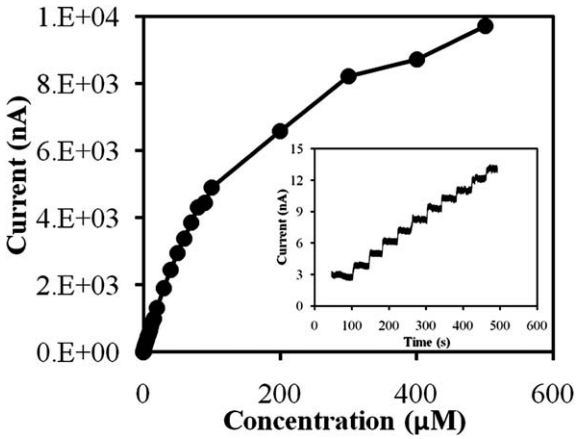

Fig. 6 The plot of response currents *versus* dopamine concentrations (the inset is a typical amperometric current response of the CNTAE on successive injection of dopamine into a stirring PBS (PH 7.2). The applied potential was set at 0.7 V and the concentration ranges from 10 nM to 100 nM).

Every individual CNT was entangled with each other, by which it supplies a large amount of additional electron transport channels, leading to a good conductive property, which is an advantage for high concentration detections.

The simple structure of the CNTAE also allows us to refresh it through mechanical polishing. Three sets of CV measurements in the μM scale have been carried out in K_3FeCN_6 and K_4FeCN_6 after simple polishing processes, and the results are shown in Fig. 5b. The linear relationships between the peak currents and the concentrations are almost identical, demonstrating a very good repeatability. This feature is very promising for biomolecular detections, in which the fouling effect[9] is frequently observed after several CV scans in normal electrodes. Other benefits of our CNTAEs may include the simple fabrication processes and potential applications for multi-functional detections. Since there is no size restriction for our CNTAEs compared to patterned electrode arrays, fabricating large area multi-channel sensor arrays becomes easier.

We also used our electrode to detect DA which is an essential neurotransmitter in the central nervous system. Determination of the dopamine level is important not only in neurobiology studies but also in the diagnosis of Parkinson's disease which is caused by the low-production of DA.[40] Fig. 6 plots the amperometric current responses of the CNTAE to different DA concentrations. The inset is a typical amperometric recording while DA is introduced into a stirring PBS (pH 7.2) at different time points to reach a final concentration from 10 nM to 100 nM. As shown, the CNTAE sensor is able to detect DA at a concentration as low as 10 nM with a signal-to-noise ratio of ~3. The linear response range spans over 4 orders of magnitude up to 100 μM. Compared to the results obtained at conventional macrosized carbon electrodes,[19,38,41] the electrochemical detection limit is enhanced.

4. Summary

A novel type of electrochemical electrode based on dense arrays of CNT open tips is demonstrated. Such electrodes can be made to an arbitrary large-size for easy fabrication and operation and,

importantly, to achieve a large detection range. It is also made up of numerous electrochemically active, low-noise, and highly conductive nanoelectrodes which offer high sensitivity. Such electrodes promise a wide range of electrochemical applications including various chemical and biological assays.

Acknowledgements

This work was supported by the Singapore MOE tier 1 RG 26/08 research fund and the NTU SUG fund.

Notes and references

1 R. H. Baughman, A. A. Zakhidov and W. A. de Heer, *Science*, 2002, **297**, 787–792.
2 P. G. Collins, K. Bradley, M. Ishigami and A. Zettl, *Science*, 2000, **287**, 1801–1804.
3 S. Ghosh, A. K. Sood and N. Kumar, *Science*, 2003, **299**, 1042–1044.
4 Y. X. Huang and P. Chen, *Adv. Mater.*, 2010, **22**, 2818–2823.
5 G. Z. Sun, S. W. Liu, K. F. Hua, X. Y. Lv, L. Huang and Y. J. Wang, *Electrochem. Commun.*, 2007, **9**, 2436–2440.
6 C. N. LaFratta and D. R. Walt, *Chem. Rev.*, 2008, **108**, 614–637.
7 R. W. Murray, *Chem. Rev.*, 2008, **108**, 2688–2720.
8 E. Bakker and Y. Qin, *Anal. Chem.*, 2006, **78**, 3965–3983.
9 M. Musameh, J. Wang, A. Merkoci and Y. H. Lin, *Electrochem. Commun.*, 2002, **4**, 743–746.
10 J. Wang, M. Musameh and Y. H. Lin, *J. Am. Chem. Soc.*, 2003, **125**, 2408–2409.
11 C. E. Banks and R. G. Compton, *Analyst*, 2005, **130**, 1232–1239.
12 C. E. Banks, T. J. Davies, G. G. Wildgoose and R. G. Compton, *Chem. Commun.*, 2005, 829–841.
13 I. W. Chiang, B. E. Brinson, R. E. Smalley, J. L. Margrave and R. H. Hauge, *J. Phys. Chem. B*, 2001, **105**, 1157–1161.
14 J. B. Xu, K. K. Hua, G. Z. Sun, C. Wang, X. Y. Lv and Y. J. Wang, *Electrochem. Commun.*, 2006, **8**, 982–986.
15 B. R. Goldsmith, J. G. Coroneus, V. R. Khalap, A. A. Kane, G. A. Weiss and P. G. Collins, *Science*, 2007, **315**, 77–81.
16 H. X. Luo, Z. J. Shi, N. Q. Li, Z. N. Gu and Q. K. Zhuang, *Anal. Chem.*, 2001, **73**, 915–920.
17 D. W. M. Arrigan, *Analyst*, 2004, **129**, 1157–1165.
18 K. S. Yum, H. N. Cho, H. Hu and M. F. Yu, *ACS Nano*, 2007, **1**, 440–448.
19 H. Cheng, W. H. Huang, R. S. Chen, Z. L. Wang and J. K. Cheng, *Electrophoresis*, 2007, **28**, 1579–1586.
20 J. Li, H. T. Ng, A. Cassell, W. Fan, H. Chen and Q. Ye, *et al.*, *Nano Lett.*, 2003, **3**, 597–602.
21 Y. Tu, Y. H. Lin and Z. F. Ren, *Nano Lett.*, 2003, **3**, 107–109.
22 D. Cai, L. Ren, H. Z. Zhao, C. J. Xu, L. Zhang and Y. Yu, *et al.*, *Nat. Nanotechnol.*, 2010, **5**, 597–601.
23 J. Hees, R. Hoffmann, A. Kriele, W. Sirnov, H. Pbloh and K. Glorer, *et al.*, *ACS Nano*, 2011, **4**, 3339–3346.
24 J. Li, J. E. Koehne, A. M. Cassell, H. Chen, H. T. Ng and Q. Ye, *et al.*, *Electroanalysis*, 2005, **17**, 15–27.
25 X. J. Huang, A. M. O'Mahony and R. G. Compton, *Small*, 2009, **5**, 776–788.
26 L. X. Zheng, G. Z. Sun and Z. Y. Zhan, *Small*, 2009, **6**, 132–137.
27 M. P. Zach, K. H. Ng and R. M. Penner, *Science*, 2000, **290**, 2120–2123.
28 E. C. Walter, M. P. Zach, F. Favier, B. J. Murray, K. Inazu and J. C. Hemminger, *et al.*, *ChemPhysChem*, 2003, **4**, 131–138.
29 J. Koehne, J. Li, A. M. Cassell, H. Chen, Q. Ye and H. T. Ng, *et al.*, *J. Mater. Chem.*, 2004, **14**, 676–684.
30 W. L. Cheng, S. J. Dong and E. K. Wang, *Anal. Chem.*, 2002, **74**, 3599–3604.
31 X. M. Liu, K. H. R. Baronian and A. J. Downard, *Carbon*, 2009, **47**, 500–506.
32 H. P. Nirmaier and G. Henze, *Electroanalysis*, 1997, **9**, 619–624.
33 W. H. Huang, D. W. Pang, H. Tong, Z. L. Wang and J. K. Cheng, *Anal. Chem.*, 2001, **73**, 1048–1052.
34 Y. Tu, Y. H. Lin, W. Yantasee and Z. F. Ren, *Electroanalysis*, 2005, **17**, 79–84.
35 Y. H. Lin, F. Lu, Y. Tu and Z. F. Ren, *Nano Lett.*, 2004, **4**, 191–195.
36 J. Shen, W. Wang, Q. Chen, M. S. Wang, S. Y. Xu and Y. L. Zhou, *et al.*, *Nanotechnology*, 2009, **20**, 245307–245316.
37 I. Dumitrescu, P. R. Unwin, N. R. Wilson and J. V. Macpherson, *Anal. Chem.*, 2008, **80**, 3598–3605.
38 J. I. Yeh and H. B. Shi, *Wiley Interdiscip. Rev.: Nanomed. Nanobiotechnol.*, 2010, **2**, 176–188.
39 N. Godino, X. Borrise, F. X. Munoz, F. J. del Campo and R. G. Compton, *J. Phys. Chem. C*, 2009, **113**, 11119–11125.
40 A. H. Liu, M. D. Wei, I. Honma and H. S. Zhou, *Adv. Funct. Mater.*, 2006, **16**, 371–376.
41 M. Lacroix, P. Bianco and E. Lojou, *Electroanalysis*, 1999, **11**, 1068–1076.